JOURNAL OF MATERIALS SCIENCE: MATERIALS IN MEDICINE 4 (1993) 481–493

Plasma-treated ultra-high-strength polyethylene fibres improved fracture toughness of poly(methyl methacrylate)

D. N. HILD*, P. SCHWARTZ
Fiber Science Program Cornell University, Ithaca, NY 14850-4401, USA

Use of ultra-high-strength polyethylene (UHSPE) fibres in composites has been limited by problems with adhesion to the matrix. The present study presents a gas-plasma treatment of UHSPE staple fibres (Spectra 900 and 1000) to improve adhesion to poly(methyl methacrylate). The gases used were nitrogen, argon and carbon dioxide for treatment times of 0 and 1 min. No significant differences were observed in flexural stresses, and only modest improvements were seen in the flexural modulus and the stress-intensity factor by reinforcing the cements with surface-modified UHSPE fibres. At least a sixfold improvement in the toughness index (fracture energy) was observed by reinforcing the cements with carbon dioxide treated fibres with a fibre index, l/d, of 776 at 1 wt %. The fibres added reinforcement by a *crack-bridging* effect that significantly improved the toughness index. The plasma treatment altered the fibre surface sufficiently to cause significant differences in the susceptibility to plastic flow during the fibre pull-out process.

1. Introduction

Acrylic-based, self-curing, bone cements – poly(methyl methacrylate) (PMMA) – have been used widely for the fixation of metallic prostheses in partial and total joint surgery since the 1950s [1, 2]. Clinical studies [3] have indicated that cement ageing and degradation (cracking) over long terms results in bulk failure and bone/cement loosening. Each year ten per cent of these surgeries are repeats due to failure [4]. With Young's moduli ratios of 100:1:10 [5] for the metal/cement/bone, clearly the weak link in the process is the poor mechanical properties of PMMA.

In recent years ultra-high-strength-polyethylene (UHSPE) fibres, Spectra, produced by Allied-Signal have become commercially available. The unique properties of Spectra lends itself to the development of composite structures with strength-to-weight ratios never before attainable. Employment of these high performance fibres, as a load-bearing component in acrylic cements, is a potential means of improving the mechanical properties of these materials. In fact, past research has included use of Spectra in PMMA with significant reinforcing effects, but no improvement in flexural strength or modulus. The weakness of the fibre/matrix interfacial bond was cited as the main problem in the composite [5].

The structural failure of fibre-reinforced materials involves three types of local failure: fibre fracture, matrix fracture and fibre–matrix interfacial bond fracture [6]. Naturally, the fibre and matrix properties are important factors in governing the strength of the composite materials, but it is the interfacial bond that ultimately determines the synergism of the fibre and matrix properties [7]. In a typical application, the load is transferred from one fibre to another via the interface and matrix. When a fibre breaks, a strong interface is needed for the redistribution of loads from the broken fibre to the surrounding fibres in the matrix.

Use of UHSPE fibres in composite applications has been hindered by the difficulties in obtaining an adequate interfacial bond between the fibre and various matrix resins, due to its polyolefin backbone. UHSPE exhibits poor wetting properties and is difficult to bond because of low surface energies, incompatibility, chemical inertness and surface contaminants. Extensive research has been conducted in the area of surface modification of polymers, including polyethylene, to alter adhesion and wettability. Employment of cold-gas plasmas has been found to significantly improve adhesion of UHSPE fibres with epoxy matrices [8–12]. Use of gas plasmas is a promising technique for improving adhesion of UHSPE fibres with PMMA matrices.

In an earlier publication we reported significantly higher interfacial shear strengths of plasma-treated UHSPE fibres with PMMA [13], based on single-fibre pull-out tests. At least a twofold improvement in adhesion was measured by treating the fibres with a gas plasma of either argon, carbon dioxide or nitrogen. One minute exposure times were found to be sufficient to cause these changes. The increased ad-

* Author to whom correspondence should be addressed, present address: Monsanto Technical Center, PO Box 97, Gonzalez, FL 32560, USA.

0957–4530

hesion was attributed to the addition of polar groups to the fibre surface, as determined by electron spectroscopy for chemical analysis (ESCA) [14]. Significant improvements in fibre wettability, as measured by contact-angle measurements, were also seen.

In this paper we report the results of using the plasma-treated fibres as reinforcement in acrylic cements. Composites were moulded, and three-point-bend loading specimens were machined and tested to obtain measurements of the flexural strength, modulus and stress-intensity factors. The toughness indices, which are a measure of fracture toughness, were also determined.

2. Experimental procedures

2.1. Fibres

UHSPE fibres, Spectra 900 (UHSPE-900) and 1000 (UHSPE-1000), with nominal fibre diameters of 38 and 28 μm, respectively, were obtained from Allied-Signal, Petersburg, VA, USA. Staple-length fibres of 6.35, 12.7 and 19.05 mm were examined. All fibres were cleaned prior to treatment to remove any processing coatings or finishes on the fibres by washing them in a 1% aqueous solution of tribasic sodium phosphate ($Na_3PO_4 \cdot 12H_2O$) in distilled water at 60 ± 3 °C for 15 min. The wash was followed by a rinse in acetone and then in distilled water. All rinses were performed at room temperature. The fibres were then air dried prior to treatment.

2.2. Acrylic bone cement

An acrylic bone cement, PMMA, was obtained from the Zimmer Corporation (Warsaw, IN, USA). The cement comprised two components, a liquid monomer and a powder polymer, which were mixed in the customary 2:1 ratio of polymer to monomer. A bone cement was selected because of its lower viscosity, which results in fewer void spaces during mixing procedures. Thus, adhesion of the fibre to the PMMA will be more complete with fewer voids. Details for mixing the cement to make fracture-toughness specimens will be discussed later.

2.3. Gas plasma

A radio-frequency-discharge plasma cleaner, model PDC-3XG (produced by Harrick Scientific Corporation, Ossining, NY, USA) was used to create the ionized gases for the fibre treatments. The electrodeless glow discharges, in this system, were generated by high-frequency oscillations introduced into the gases by means of solenoid coils wrapped around the outside of the plasma chamber. The plasma chamber was of Pyrex glass. The induction coils were connected to a radio-frequency (RF) generator at 13.56 MHz, which supplied the high-frequency currents to excite the gas inside the chamber and form the plasma.

Fibres were exposed to a gas plasma of either argon, nitrogen or carbon dioxide at a power level of 30 W, which was the maximum power wattage of our plasma system. Argon was selected because it is an inexpensive inert gas that is commonly used as a flow gas in plasmas. Nitrogen has the potential for creating amines on the surface of the fibres. Carbon dioxide was selected because it is rich in oxygen without having the safety problems of a pure oxygen gas – pure oxygen is highly explosive. Oxygen plasmas are well known to be an aggressive treatment for polymers. The chamber was evacuated to < 20 Pa before introduction of the gas. The chamber was flooded with the gas to > 600 Pa. The chamber was then re-evacuated to 33 Pa. The flow rate of the gas was kept constant, so that a pressure of 33–40 Pa was maintained. Fibres were then exposed for 1 min with unexposed fibres used as controls. In a previous paper [13] we found under these operating conditions that 1 min exposure was sufficient to cause significant improvements in interfacial-shear strengths and fibre pull-out energies.

2.4. Scanning electron microscopy

A JEOL scanning electron microscope (SEM) model JSM 35 CF was used to observe the surface topography of treated and control fibres, as well as the fibres pulled out from the PMMA matrix. It was also used to observe the bonding between the fibre and cement and the voids in the PMMA surface. Fibre distributions within the fracture specimens were also examined. Specimens were coated with a 60/40 gold/palladium alloy using a pulse-plasma system. Samples were examined in the SEM using an accelerating voltage of 5 kV. UHSPE fibres were very easily damaged by the electron-beam radiation in the SEM and, thus, it was necessary to maintain the voltage as low as possible.

2.5. Fracture toughness

Standard three-point bend fracture toughness (ASTM Standard D-790) specimens were moulded using 6.35 and 1.27 mm lengths of UHSPE-900 fibres and 6.35 and 19.05 mm lengths of UHSPE-1000 fibres. These fibres were mixed into PMMA powder at 0.5 and 1 wt % concentrations prior to mixing with the liquid monomer. To ensure a more uniform distribution of fibre within the matrix, the PMMA powder was first fractionated into four equal portions before introducing the UHSPE staple fibres. Equal proportions of fibre were added to the fractionated powder to form a weight percentage of either 0.5 or 1%. The polymer powder and fibre were mixed by hand, after which all fractions were combined. Liquid monomer was added to the powder/fibre mixture and the cement was stirred by hand at room temperature using the 2:1 powder-to-liquid ratio. The cement mixture was poured into a silicon-rubber mould with plate dimensions of $12 \times 10.5 \times 0.8$ cm^3. The polymer was compressed in the mould by placing a weight of 2254 N on top of the composite. The weighted moulds were placed in a circulating-air oven at 37 °C and allowed to cure for at least 24 h before removing the plates from the moulds. The curing time and temperature was selected to simulate actual temperatures *in vivo*.

After removing the PMMA from the mould, three-point bend test beams ($0.5 \times 0.6 \times 5$ cm^3) were ma-

chined from the plates and sharp notches of 0.24 cm depth (Fig. 1. $a/w = 0.4$) were inserted using a saw-tooth-edge-solid-carbide circular blade. All specimens were conditioned (21 °C, 65% relative humidity (r. h.)) for at least 48 h, prior to testing. Notched and unnotched specimens were tested in a three-point bend loading with a span of 2.54 cm using an Instron Model 1122 testing machine, at a displacement rate of 5 mm min^{-1}. The sample size was six specimens per data point in all cases. The flexual strengths, σ_f, of the unnotched specimens were computed using the ASTM Standard D-790 formula:

$$\sigma_f = \frac{3FL}{2bw^2} \quad (1)$$

where F is the maximum load, and b, w and L are shown in Fig. 1. The ratio $w/l = 0.12$, which means that simple bending theory does not apply, thus a shear correction factor described by Timoshenko and Goodier [15] was used to calculate the flexural modulus, E_f:

$$E_f = K\left(\frac{L}{4bw^3}\right)\left[1 + 2.85\left(\frac{w}{L}\right)^2 - 0.84\left(\frac{w}{L}\right)^3\right] \quad (2)$$

where K is the slope at the origin of the load–displacement graph. The fracture toughness, K_{IC}, was computed using the following expression, derived from linear fracture mechanics [16]:

$$K_{IC} = \left(\frac{3FLa^{1/2}}{2bw^2}\right) Y\left(\frac{a}{w}\right) \quad (3)$$

where F is the maximum load, a is the notch depth and b is the beam thickness. Y is defined as follows, for span-to-depth ratios of 4 (which is the case here):

$$Y\left(\frac{a}{w}\right) = 1.93 - 3.07\left(\frac{a}{w}\right) + 14.53\left(\frac{a}{w}\right)^2 - 25.11\left(\frac{a}{w}\right)^3 + 25.8\left(\frac{a}{w}\right)^4 \quad (4)$$

3. Results and discussion

3.1. Scanning electron microscopy

Figs 2–5 are SEM photomicrographs of notched specimens that were fractured in the three-point bend loading test. The distribution of the fibres within the matrix was fairly uniform for all fibre aspect ratios and weight fractions. No "bundling" of fibres was apparent, which is in agreement with other reports in the literature [5, 17]. Fibre bundling of UHSPE fibres essentially reduces the amount of reinforcement from the fibres [18] because the PMMA would not be in total contact with all the fibres within the bundle. None of the fibres appears to be broken; thus, failure

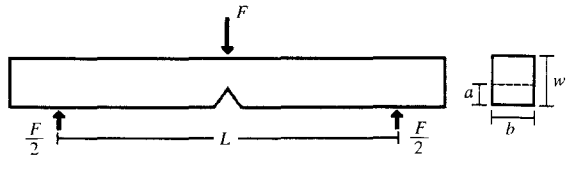

Figure 1 Schematic of a three-point bend loading specimen.

Figure 2 Surface topography of a fractured three-point bend loading test specimen reinforced with UHSPE-1000 virgin fibres of 6.35 mm lengths at 1 wt % fraction.

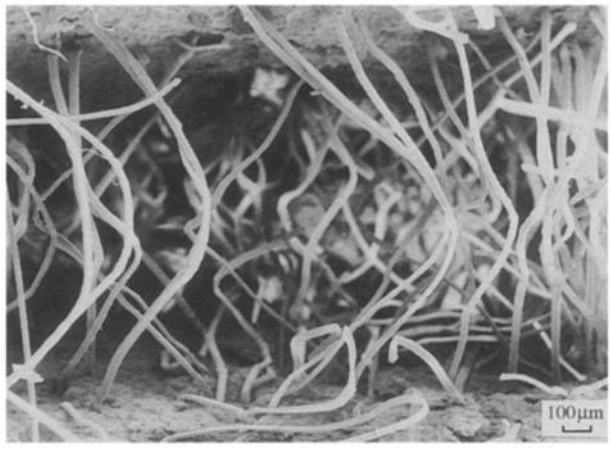

Figure 3 Surface topography of a fractured three-point bend loading test specimen reinforced with nitrogen plasma-treated UHSPE-1000 fibres of 19.05 mm lengths at 1 wt % fraction.

Figure 4 Surface topography of a fractured three-point bend loading test specimen reinforced with argon plasma-treated UHSPE-900 fibres of 6.35 mm lengths at 1 wt % fraction.

in these specimens occurred from the low interfacial-bond strength between fibre and matrix, as seen by fibre pull-out in these specimens. This was not surprising since the maximum fibre length in most of the specimens was less than the critical fibre length, as

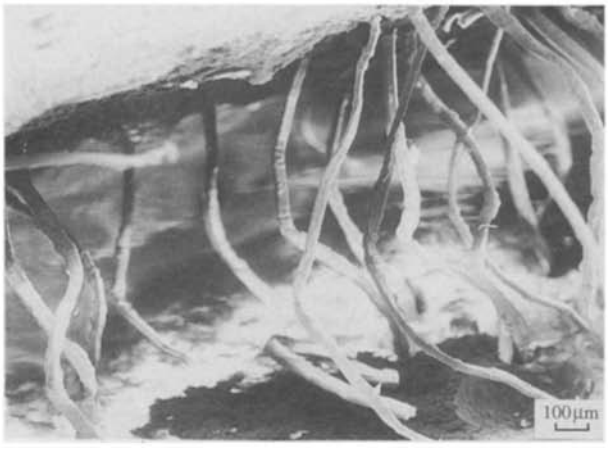

Figure 5 Surface topography of a fractured three-point bend loading test specimen reinforced with carbon dioxide plasma-treated UHSPE-900 fibres of 12.7 mm lengths at 0.5 wt % fraction.

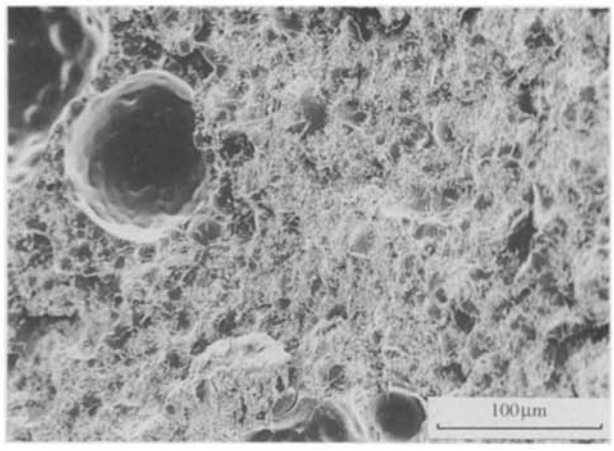

Figure 6 Surface topography of a fractured three-point bend loading test specimen that is unreinforced.

formulated by Wang [18]:

$$L_c = \frac{d_f \sigma_f}{4\tau} \quad (5)$$

where L_c is the critical fibre length, d_f is the nominal fibre diameter, σ_f is the fibre strength, and τ is the interfacial-shear strength.

The calculated critical fibre length, L_c, for a UHSPE-900 fibre, assuming $d_f = 36$ μm, $\sigma_f = 3400$ MPa and $\tau = 1.5$ MPa is 20.4 mm in length. The maximum length of UHSPE-900 fibres in this study was 12.7 mm. It should be noted that the maximum length of UHSPE-1000 fibres (19.05 mm) was greater than the calculated L_c (11.7 mm), assuming $d_f = 26$ μm, $\sigma_f = 3600$ MPa and $\tau = 2$ MPa. In order to achieve a maximum reinforcement effect from the fibres, it appears that an increase in interfacial shear strength or longer fibres may be needed, as the failure mechanism in the specimens was by fibre pull-out, rather than fibre breakage. It should be noted that longer fibres may cause problems in mixing procedures. Piggott [19] stated that even with "good" adhesion, fibre pull-out would be observed because of the extremely large shear stresses at the fibre–matrix interface.

The surface topography of a fractured specimen without fibre reinforcement can be seen in Fig. 6. Voids are apparent throughout the cement.

A magnified view of the fibres reveals pieces of PMMA remaining on the fibre surface (Fig. 7). From the photomicrographs, there were no observed differences between the controls and the plasma-treated fibres in the amount of PMMA found on the fibre surfaces. Larger amounts of PMMA were seen at surface defects along a fibre length, such as areas around *kink bands* (Fig. 8) (using the terminology of Smooks *et al.* [20] and Schwartz *et al.* [21]) which was expected. All fibres showed signs of plastic flow, which occurred as fibres slipped through the matrix (Figs 8 and 9), which agrees with Davy *et al.* [22]. Noticeable platelettes were formed on the surface of both the controls and the treated fibres. The platelettes were always directed towards the PMMA surface, which suggests that they were formed during pull-out. This confirms earlier findings of possible surface abrasion seen in the SEM photomicrographs taken of fibre pull-out specimens [13].

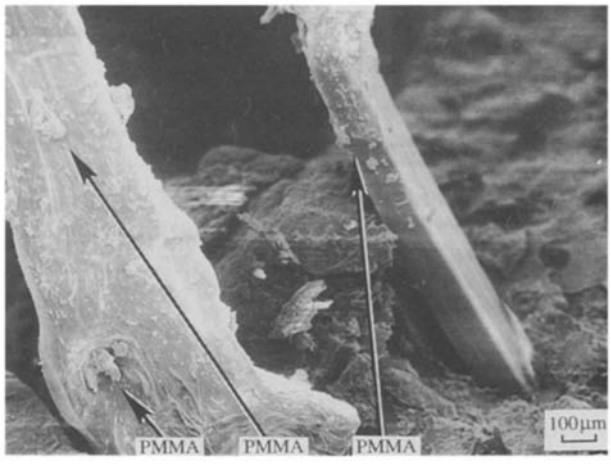

Figure 7 A magnified view of the surface topography of fibres (argon-treated UHSPE-900 of 6.35 mm length at 1 wt % fraction) within a fractured three-point bend loading test specimen.

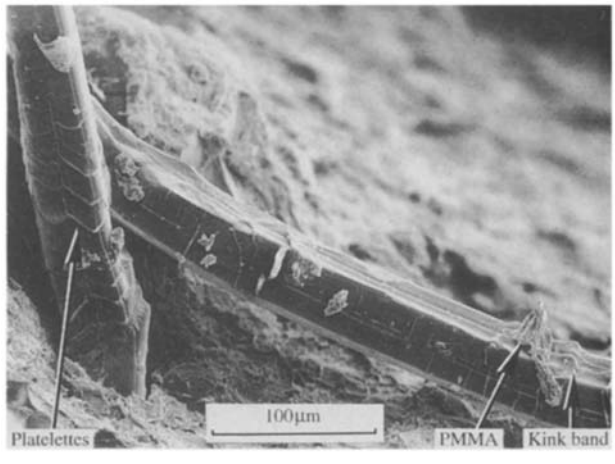

Figure 8 A magnified view of the surface topography of fibres (virgin UHSPE-1000 fibres of 6.35 mm length at 1 wt % fraction) within a fractured three-point bend loading test specimen.

3.2. Mechanical-test results

Means obtained from the three-point bend loading tests are reported in Table I. Values listed are from

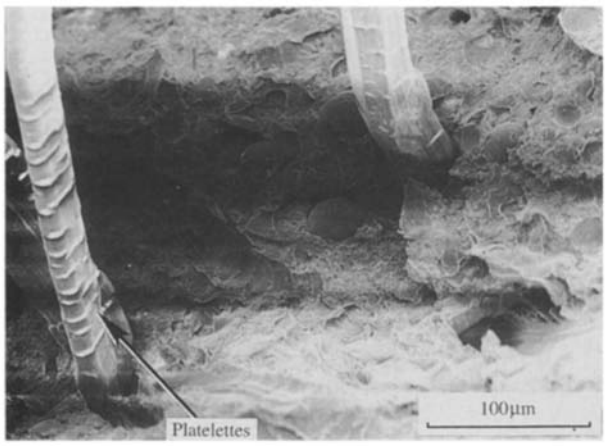

Figure 9 A magnified view of the surface topography of fibres (carbon-dioxide-treated UHSPE-900 fibres of 6.35 mm length at 0.5 wt % fraction) within a fractured three-point bend loading test specimen.

a minimum of five data points for each condition. The fibre aspect ratios that are listed refer to the following combinations: UHSPE-900 fibres of 6.35 mm lengths (and an aspect ratio of 188), UHSPE-1000 fibres of 6.35 mm lengths (244), UHSPE-900 of 12.7 mm lengths (372), and UHSPE-1000 of 19.05 mm lengths (776). A three-way analysis of variance was used to test for equality of means ($\alpha = 0.05$). The independent variables of the plasma gas, fibre aspect ratio (fibre length/fibre nominal diameter), and weight percentage, as well as their interactions, were examined to determine their effect on the flexural strength, σ_f, the flexural modulus, E_f, and the stress-intensity factor, K_{IC}. From the statistical analysis, the independent variables of the plasma gas and weight fraction, and an interaction between the plasma gas and weight fraction, were found to be significant factors in determining K_{IC}. The independent variable of the type of plasma gas was also found to be a significant factor for determining E_f. No other statistically significant differences were found in these data at $\alpha = 0.05$. Means for each of the dependent variables as a function of the plasma gas are reported in Table II.

3.3. Flexural strength

The means ($\pm$ one standard error) that were obtained for flexural strengths, σ_f, of unreinforced and reinforced cements by weight percent are presented in Fig. 10. Little or no reinforcing effect in σ_f was realized by incorporating the fibres into the cement, regardless of the treatment condition. These results were not unexpected, as Wagner and Cohn [17] examined composites of bone cements reinforced with 1 wt % UHSPE-900 fibres that were treated with an oxygen plasma and also fibres grafted with methyl-methacrylate monomer without finding an improvement in σ_f. A poor fibre–matrix interfacial adhesion, even with the surface-treated fibres, was the conclusion drawn for the decrease in mechanical properties seen by these researchers. They conjectured that, because of the weak fibre–matrix adhesion, the fibre content of UHSPE-900 fibres within the cement could be equated with the void concentration. Wagner and Cohn recommended harsher fibre-surface treatments to improve the interfacial bond to obtain any benefit from UHSPE-900 fibres. It should be noted that they did not measure the interfacial shear strength of the treated and untreated fibres in their study.

Interlaminar-shear strength (ILSS) and three-point-bend loading tests were performed on plasma-treated UHSPE-900 and UHSPE-1000 fabrics embedded in an epoxy matrix by Kaplan *et al.* [10]. In this study a fourfold increase in ILSS was seen by the researchers, but only a modest improvement was found in the flexural strength and modulus. Kaplan *et al.* stated that interfacial adhesion influences ILSS more strongly than it influences flexural properties in tests where the span-to-depth ratio is small, $l/w < 16$,

TABLE I The means of flexural strength, σ_f, flexural modulus, E_f, and the stress-intensity factor, K_{IC}, for UHSPE/PMMA composites

Gas	Fibre aspect	σ_f (MPa)		E_f (GPa)		K_{IC} (MPa m$^{1/2}$)	
	ratio, $1/d$	0.5 wt %	1.0 wt %	0.5 wt %	1.0 wt %	0.5 wt %	1.0 wt %
No fibre	0	58.0	58.0	1.72	1.72	0.81	0.81
Control	188	59.0	58.8	2.65	2.64	0.92	1.12
	244	55.5	54.2	2.64	2.48	0.95	0.99
	372	55.3	54.9	2.04	2.58	1.00	0.89
	776	58.1	60.0	2.53	2.37	0.97	1.06
Argon	188	60.7	59.3	2.61	2.42	0.97	0.88
	244	51.1	62.7	2.38	2.77	1.03	1.31
	372	59.3	52.4	2.26	2.06	0.88	0.98
	776	57.9	57.2	2.28	2.98	0.87	0.96
Carbon dioxide	188	60.8	58.6	2.37	2.63	1.07	1.16
	244	63.5	59.2	2.92	2.66	1.06	0.98
	372	62.2	58 9	2.46	2.81	1.01	1.08
	776	59.3	61.9	3.22	2.93	1.07	1.04
Nitrogen	188	57.7	59.1	2.35	2.44	0.91	1.12
	244	63.8	58.1	3.08	2.29	0.96	1.07
	372	57.5	58.9	2.67	2.81	0.87	1.08
	776	57.0	58.3	2.64	2.68	0.97	1.15

TABLE II Means of the flexural strength, σ_f, flexural modulus, E_f, and stress-intensity factor, K_{IC}, for UHSPE/PMMA composites for different gases (values are combined for all weight fractions and fibre aspect ratios)

Gas	σ_f (MPa) (CV%)	E_f (GPa) (CV%)	K_{IC} (MPa m$^{1/2}$) (CV%)
No fibre	58.0[a]	1.72[a]	0.81[a]
	(24.5)	(24.9)	(8.2)
Control	57.0[a]	2.49[b]	0.99[b, c]
	(14.1)	(21.3)	(15.6)
Argon	57.8[a]	2.51[b]	0.97[b]
	(13.1)	(28.8)	(17.6)
Carbon dioxide	60.5[a]	2.76[b]	1.06[c]
	(8.5)	(21.5)	(11.0)
Nitrogen	58.9[a]	2.64[b]	1.01[b, c]
	(12.1)	(22.4)	(17.3)

[a-c] The different letters by column represent significantly different means at $\alpha = 0.05$.

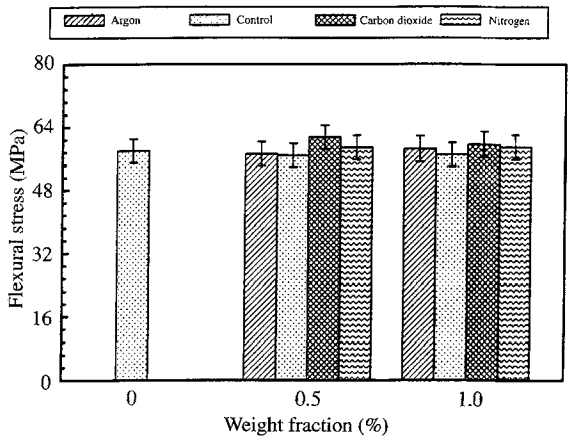

Figure 10 Flexural stress (means ± one standard error) for fibre-reinforced and unreinforced cements as a function of weight percentage (values are combined for virgin and plasma-treated fibres).

using Fig. 1 as a reference. They suggested that a mixed mode of failure (compressive, tensile and shear) is experienced by the specimens when a small span-to-depth ratio is used following the ASTM D–790 standard test method. In our study no significant differences were observed in the flexural-strength measurements obtained from the three-point bend loading tests, in spite of the significant increase in adhesion seen in the plasma-treated fibres that we reported in an earlier paper [13]. A small span-to-depth ratio ($l/w \approx 4$) was used for testing the specimens, which could account in part for the lack of observed differences in the flexural-strength properties in our experiment. Since failure in the reinforced cements was dominated by fibre pull-out rather than by breaking of the fibres, a poor interfacial-shear strength could be another reason for the lack of observed differences in these specimens.

3.4. Flexural modulus

In Fig. 11, the means (± one standard error) obtained from the flexural modulus, E_f, of unreinforced and reinforced cements, as a function of the plasma gas used are presented. Clearly, significant improvements

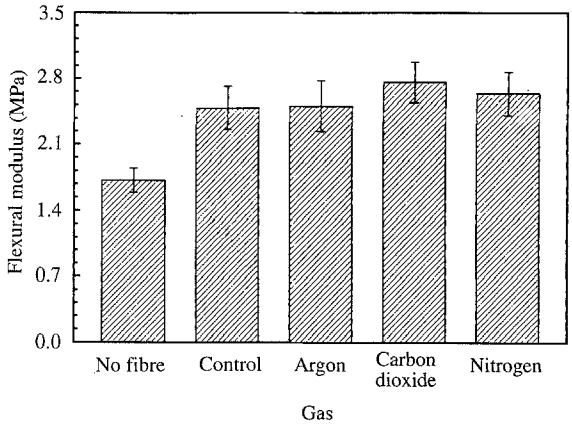

Figure 11 Flexural modulus (means ± one standard error) as a function of the plasma gas used (values are combined for weight fractions and fibre aspect ratios).

in E_f were realized for all fibre-reinforced specimens over non-reinforced cements, although the magnitude of improvement is modest. The fibre-reinforced samples have a flexural modulus that is 1.5 times stiffer than the unreinforced specimens. No statistically significant differences in flexural modulus were observed among the fibre-reinforced specimens ($\alpha = 0.05$), although it should be noted that the mean obtained from cements reinforced with carbon dioxide treated fibres had the highest observed flexural modulus.

The results of our study conflict with other results reported in the literature. Reductions in stiffness for UHSPE-reinforced bone cements were observed by other researchers [5, 17] for both untreated and surface-modified (by gas plasmas) UHSPE at weight percentages of 1, 4 and 7%. It was concluded in the previous studies that UHSPE fibres, due to their poor adhesion with PMMA, act as voids within the cement, essentially reducing the modulus of the material. The inclusion of fibres in our study did improve the stiffness of the cements; although the improvement was modest.

3.5. Stress-intensity factor

Means (± one standard error) for K_{IC} as a function of the plasma gas can be seen in Fig. 12. A modest, but statistically significant, improvement in K_{IC} was seen by reinforcing the cements with fibres. The reinforcing effect of fibres, even those exposed to a plasma treatment, was weak, which is in agreement with other results in the literature [5, 17]. In fact, Wagner and Cohn [17] concluded that even with plasma-treated fibres the reinforcing effect was so weak that it was doubtful whether this approach would yield any benefit in the mechanical behaviour, unless harsher fibre-surface treatments were utilized.

The carbon dioxide specimens had a significantly higher K_{IC} than the argon specimens. No other significantly different means as a function of the plasma gas were seen in these data. Carbon dioxide is known to be a harsher treatment than nitrogen and argon, due to the oxygen-rich environment within the plasma chamber. We reported in a previous paper [14] that argon plasma treatments require much longer

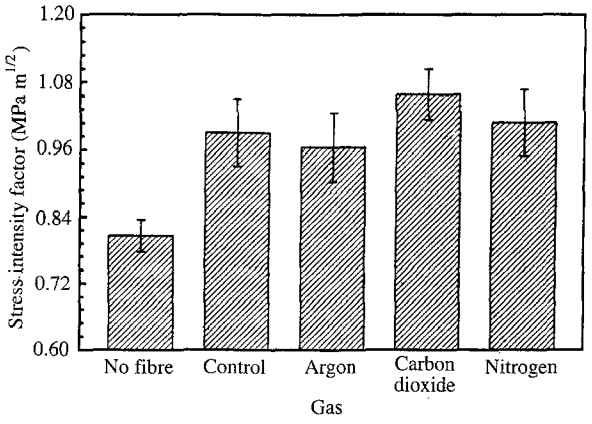

Figure 12 K_{IC} (means ± one standard error) for fibre-reinforced and unreinforced cements as a function of the plasma gas (values are combined for weight fractions and fibre aspect ratios).

exposure times to achieve similar improvements in the wettability of polymer films in comparison to both nitrogen and carbon dioxide. Although there were no significant differences in the observed wettability of plasma-treated UHSPE fibres, it is probable that the carbon dioxide plasma treatment improved the wettability of UHSPE fibres to the extent that adhesion to PMMA was enhanced sufficiently to realize a difference between argon plasmas and carbon dioxide plasmas.

K_{IC} values as a function of weight fraction are given in Table III and in Fig. 13. A modest, but significant, improvement in K_{IC} was seen in all fibre-reinforced specimens compared to the unreinforced specimens. This was expected, as modest improvements in K_{IC} by reinforcing bone cements with UHSPE fibres at weight fractions of 1% have been reported in the literature [5, 17]. There were no observed differences between the two weight fractions in the reinforced specimens. Apparently, little benefit is gained by having a weight percentage of 1% compared to 0.5% in the observed values of K_{IC}.

K_{IC} values as a function of the interaction between the plasma gas and the weight fraction are given in Table IV and in Fig. 14. The carbon dioxide treatment yielded significantly higher K_{IC} values at both weight fractions in comparison to most of the treatments. Nitrogen treated fibres at a 1% weight fraction were significantly higher than most of the treatments. As mentioned previously, both carbon dioxide and nitrogen are more rigorous treatments at a 1 min exposure time than the argon treatment.

From the SEM photomicrographs it was concluded that fibre pull-out was part of the failure mechanism in the reinforced specimens because broken fibres were not observed in the specimens. (Matrix cracking was the primary mechanism of failure.) Since there were no significant differences in the K_{IC} means obtained from the analysis of fibre aspect ratio, the weakness of the fibre–matrix interfacial bond was apparently the dominating mechanism for fibre debonding in these specimens. The longer fibres did not require a higher force for debonding. More intense plasma treatments may be needed to realize any benefit in the fracture-

TABLE III Means of the stress-intensity factor, K_{IC}, as a function of weight fraction (values are combined for all plasma-treated and virgin fibres, and fibre aspect ratios)

Weight fraction (%)	K_{IC} (MPa m$^{1/2}$)	CV (%)
0	0.81 [a]	8.19
0.5	0.97 [b]	11.2
1.0	1.04 [b]	18.0

[a, b] The different letters represent significantly different means at $\alpha = 0.05$.

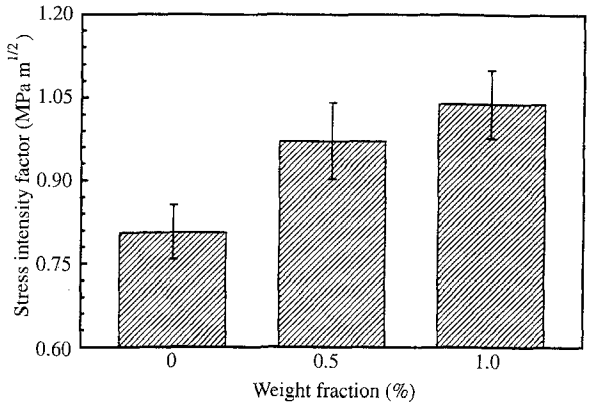

Figure 13 K_{IC} (means ± one standard error) for fibre-reinforced (values are combined for all plasma-treated fibres and fibre aspect ratios) and unreinforced cements as a function of the weight fraction.

TABLE IV Means of the stress-intensity factor, K_{IC}, as a function of the interaction of the gas with the weight fraction (values are combined for all fibre aspect ratios)

Gas	Weight fraction (%)	K_{IC} (MPa m$^{1/2}$)	CV (%)
No fibre	0	0.81[a]	8.2
Controls	0.5	0.97[b, c]	12.8
	1.0	1.02[c, d, e]	15.9
Argon	0.5	0.94[a, b, c]	12.0
	1.0	0.97[b, c]	16.2
Carbon dioxide	0.5	1.05[c, d, e]	10.0
	1.0	1.07[d, e]	11.5
Nitrogen	0.5	0.93[a, b]	10.9
	1.0	1.10[e]	16.3

[a – c] The different letters represent significantly different means at $\alpha = 0.05$.

toughness performance of these bone cements by reinforcement with UHSPE fibres.

4. Frictional-energy in composites

4.1. Frictional-energy analysis

In reviewing the literature on fibre-reinforced bone cements, the analysis of mechanical properties has been limited to measurements of σ_f, E_f, K_{IC} and J-integrals. All of these measurements only account for the initial portion of the stress-strain curve, where catastrophic failure of the cement supposedly occurs. From general observations during the actual testing of

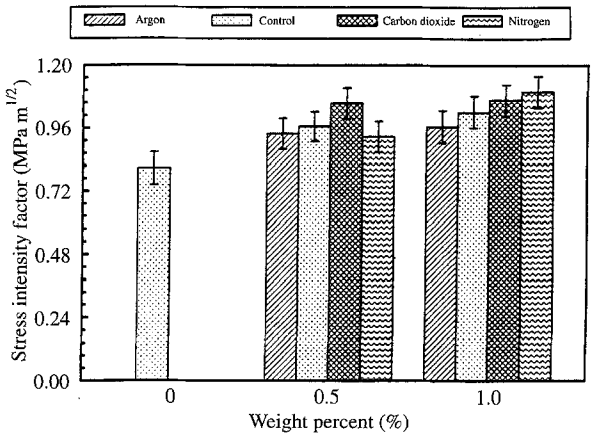

Figure 14 K_{IC} (means ± one standard error) for fibre-reinforced and unreinforced cements as a function of the weight fraction and the plasma gas (values are combined for all fibre aspect ratios).

specimens, there were very noticeable differences between the behaviour of the reinforced and unreinforced specimens after the failure criterion was met, which was indicated by a dramatic load drop. Noticeable differences were not seen during the initial portion of the test, but at the catastrophic failure point, all of the unreinforced specimens broke into two fragments almost instantaneously; whereas, a *crack bridging* by the fibres was seen in all of the reinforced samples.

In Fig. 15 we present typical load–elongation curves obtained from the three-point bend loading test of an unreinforced specimen, a reinforced specimen with control fibres and a reinforced specimen with plasma-treated fibres. In the unreinforced specimen, the load dropped to zero when failure occurred; the crack had propagated through the entire specimen. Catastrophic failure of the unreinforced cement is determined because the cement is broken into two or more fragments, which would indicate failure of the construct in an *in vivo* situation. This is when the test method is essentially complete for measuring the parameters σ_f, E_f, K_{IC} and the J-integral. The fibre-reinforced specimens continued to bear a load after the crack had propagated through the specimen. In fact, the load-bearing capacity of the cement actually increased in some of the specimens (Fig. 15c), which is very similar to observations of the load–elongation curves obtained from the single-fibre pull-out tests of plasma-treated fibres [13]. A very significant reinforcement effect was obtained from the fibres after the failure criterion of the bone cements was determined, because the fibres actually hold the pieces together, improving the load-bearing capacity of the cement. This *bridging effect* goes entirely unnoticed if one only examines the parameters σ_f, E_f and K_{IC}. In fact, other researchers have concluded that only modest improvements in the measured values for K_{IC} and E_f were obtained from reinforcement of the cements by UHSPE fibres [5, 17]. They stated that the improvement was so weak it was doubtful whether this approach would yield any benefit in the mechanical behaviour of acrylic bone cements. Clearly a benefit in the mechanical properties by fibre reinforcement is

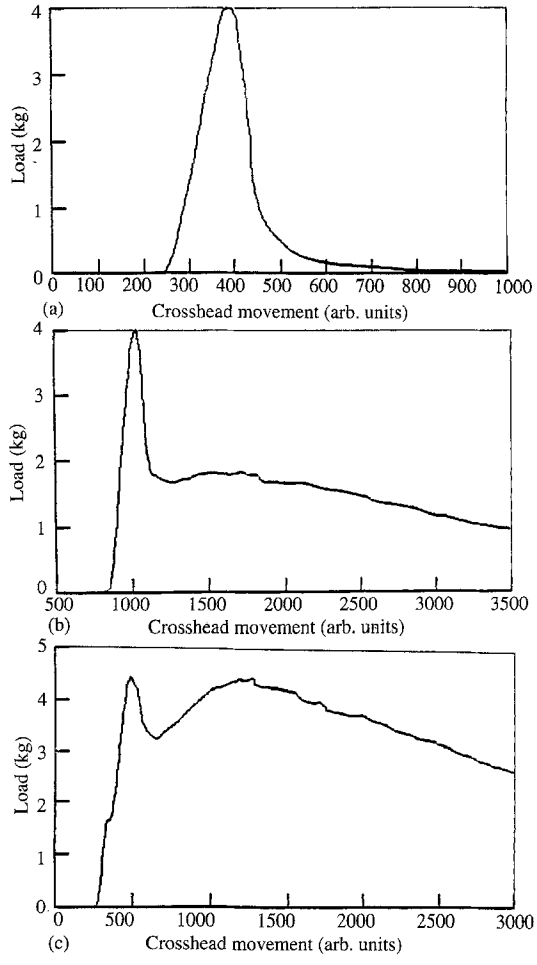

Figure 15 Typical load–elongation curves obtained from the three-point-bend loading test for: (a) an unreinforced cement, (b) a cement reinforced with virgin UHSPE fibres, and (c) a cement reinforced with UHSPE plasma-treated fibres.

realized if one examines the load–elongation curves of the entire test; the energy obtained from load–elongation curves should be included in the analysis.

When a crack has propagated through the entire unreinforced specimen, catastrophic failure results. For the fibre-reinforced specimens, when a crack has propagated through the entire specimen elastic debonding between the fibre and matrix has taken place. However, in order for complete failure to occur, slippage of the fibre through the matrix also needs to happen. The measured parameters discussed above ignore this reinforcement effect, when it is essentially a key factor for improving the lifetimes of the cements. In order for the effect of fibre reinforcement to be fully realized, the results of the frictional forces from fibre slippage also need to be included in the analysis.

4.2. Toughness index analysis

In a previous paper [13] it was argued that fibre pull-out can be divided into two components, the stress needed for elastic debonding and the stress needed for slippage of the fibre through the matrix. One method for analysing the frictional effect is to examine the energy needed for fibre slippage (toughness index). Several methods have been proposed for measuring the toughness indices (TIs) obtained from ASTM

D–790 fracture-toughness tests. The toughness-index method selected to analyse these data was a modification of the secant method (Fig. 16a) that was proposed by Wang [18]. To obtain the secant line Wang proposed multiplying the initial compliance by 20. For this analysis the compliance was multiplied by 40 (Fig. 16b), in order to include a larger portion of the area under the curve, as much of this information would be lost if the compliance was multiplied by 20. For determining S_0, as defined in Fig. 16, the area was calculated from the point in the graph where there was a dramatic load drop, due to the crack propagation across the entire specimen. Based on this calculation, the TI of the unreinforced specimens was set equal to 1.0 because the load dropped to zero at this point.

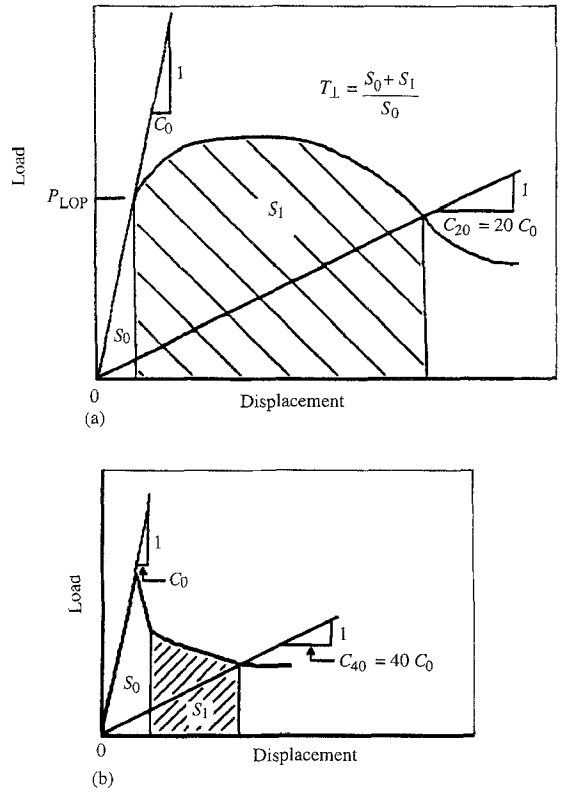

Figure 16 A toughness index based on: (a) the secant compliance, C_0 = initial specimen compliance, $C_{20} = 20C_0$, toughness index = $(S_0 + S_1)/S_0$ [18]; and (b) the modified secant compliance, C_0 = initial specimen compliance, $C_{40} = 40C_0$, toughness index = $(S_0 + S_1)/S_0$.

Values obtained from calculating the TI (from a minimum of five data points for each condition) are given in Table V. A three-way analysis of variance was performed on these data to test for the equality of means ($\alpha = 0.05$). The independent variables of the plasma gas, fibre aspect ratio, and weight percentage, as well as their interactions, were examined to determine their effect on the toughness index.

4.3. Toughness index as a function of the plasma gas

A summary of TI tabulated by gas treatment is given in Table VI and can also be seen in Fig. 17. All plasma-treated fibre-reinforced specimens had at least a threefold improvement in TI in comparison to the unreinforced specimens. Significantly higher TI were observed in the cements reinforced with plasma-treated fibres, regardless of the gas used, in comparison to the cements reinforced with virgin fibres. There were no significant differences among the three gases in the TI that were obtained in these data.

Earlier it was reported that there were no significant differences in the values of σ_f, E_f or K_{IC} observed between the cements reinforced with plasma-treated fibres and those reinforced with virgin fibres. The surfaces were not altered sufficiently to cause noticeable discrepancies in the fibre-debonding process.

TABLE V Toughness index means for UHSPE/PMMA composites

Gas	Weight fraction (%)	Toughness index			
		Fibre aspect ratio, l/d			
		188 (CV%)	244 (CV %)	372 (CV %)	776 (CV %)
No fibre	0	1.0	1.0	1.0	1.0
		–	–	–	–
Control	0.5	1.86	1.82	2.11	2.85
		(12.0)	(14.7)	(13.0)	(19.5)
	1.0	2.36	2.64	2.74	3.54
		(19.2)	(18.1)	(20.9)	(30.8)
Argon	0.5	2.13	2.60	2.54	4.35
		(15.7)	(18.8)	(22.1)	(19.2)
	1.0	3.10	4.16	3.51	4.17
		(20.7)	(20.8)	(23.7)	(18.4)
Carbon dioxide	0.5	1.80	2.67	2.70	4.27
		(14.5)	(37.7)	(14.0)	(17.4)
	1.0	2.83	3.36	3.67	6.82
		(7.2)	(12.7)	(29.4)	(79.8)
Nitrogen	0.5	1.87	2.23	3.71	4.01
		(8.7)	(5.4)	(17.9)	(39.8)
	1.0	3.36	2.87	3.47	5.80
		(34.5)	(19.4)	(16.7)	(7.2)

TABLE VI Toughness index means as a function of the gas treatment used (values are combined for all weight fractions and fibre aspect ratios)

Gas	Toughness index	CV (%)
No fibre	1.00[a]	–
Control	2.42[b]	29.3
Argon	3.30[c]	31.1
Carbon dioxide	3.48[c]	50.2
Nitrogen	3.38[c]	39.5

[a–c] The different letters represent significantly different means at $\alpha = 0.05$.

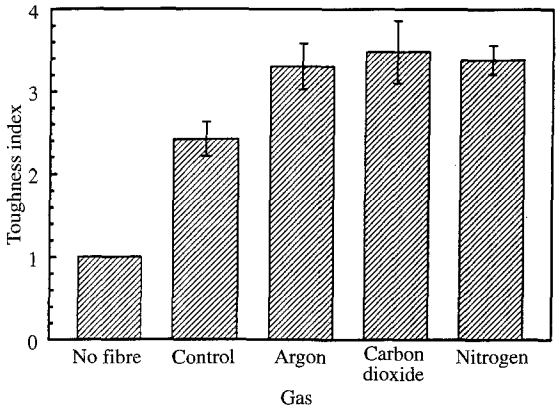

Figure 17 Toughness index (means ± one standard error) as a function of the plasma gas (values are combined for all weight fractions and fibre aspect ratios).

However, significant differences were observed in the frictional forces needed to pull specimens from the matrix. The plasma treatment is known to be a surface phenomena that preferentially attacks the less-oriented amorphous regions in the fibres. It is possible that the plasma-treated fibres were more susceptible to plastic flow during fibre pull-out because of these surface changes. This would cause an increase in the amount of friction needed to pull the plasma-treated specimens through the matrix. In fact, the highest TI was observed on the fibres exposed to carbon dioxide, which is considered to be the most aggressive of the three gases examined, although these data were not significantly different from the argon or nitrogen treatments, probably due to the large coefficient of variation (CV) observed in these data. The means were calculated by averaging all of the weight fractions and fibre aspect ratios together. The carbon dioxide fibres had an extremely large spread in the data when examining the data points for the lower aspect ratios and weight fractions in comparison to the highest fibre aspect ratio and weight fraction. This would account for the extremely large CV observed in these data.

It should be possible to explore this hypothesis more thoroughly by examining the distance between platelettes of the treated fibres in comparison to the controls. Unfortunately, due to the random distribution of fibres, the fibres in this experiment were aligned at many different angles within the matrix and it was difficult to obtain accurate measurements from the SEM photomicrographs. Thus, no conclusive data were found. In order to analyse this hypothesis more thoroughly, the fibre alignment would need to be controlled.

Clearly, from this analysis, a significant improvement in the mechanical properties of the cements was obtained from reinforcing PMMA with plasma-treated fibres. This reinforcement is obtained from the *bridging effect* that the fibres impart after a crack has propagated across the cement. The plasma-treated fibres were more difficult to pull from the matrix, as seen by the TI measurements.

4.4. Toughness index as a function of the weight fraction

A summary of TI as a function of weight fraction is given in Table VII, and can also be found in Fig. 18. Significantly higher TIs were observed for the specimens reinforced by fibres at 1.0 wt % in comparison to those reinforced at 0.5 wt %. As stated above, all fibre-reinforced specimens had significantly higher TIs in comparison to the unreinforced specimens. The weight fractions selected for this experiment were based on the results of previous research [5, 17, 23, 24] suggesting that higher weight fractions essentially reduced σ_f, E_f and K_{IC} because the fibres acted as voids within the cement. No significant differences were observed between the two weight fractions in the means obtained for σ_f, E_f and K_{IC} in the present research. Apparently, the different weight percentages examined in this experiment did not make a difference in the load needed for elastic debonding, but a significant reinforcement effect was observed by the increased energy needed for fibre slippage with the higher per-

TABLE VII Toughness index means as a function of weight fraction (values are combined for all virgin and plasma-treated fibres)

Weight fractions (%)	Toughness index	CV (%)
0	1.0[a]	–
0.5	2.71[b]	18.2
1.0	3.61[c]	23.3

[a–c] The different letters represent significantly different means at $\alpha = 0.05$.

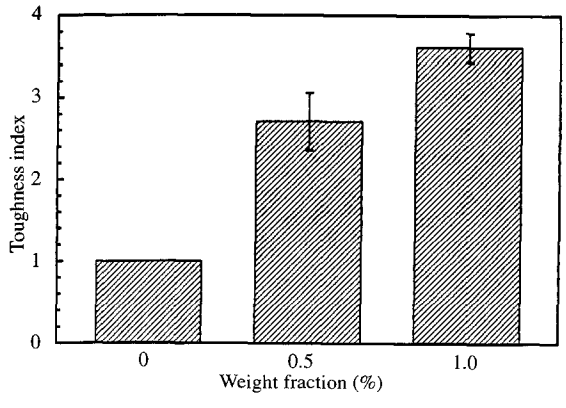

Figure 18 Toughness index (means ± one standard error) as a function of weight fractions (values are combined for all virgin and plasma-treated fibres, and for all fibre aspect ratios).

centage of fibres. From the SEM photomicrographs presented earlier in this paper, plastic flow was observed on all of the fibre surfaces in the form of platelettes, due to fibres being pulled through the matrix. It is postulated that the larger amount of fibre within the matrix, especially when it is abraded, caused an increase in the amount of frictional forces needed to pull the fibre from the PMMA.

4.5. Toughness index as a function of the fibre aspect ratio

A summary of TI as a function of fibre aspect ratios is given in Table VIII, and can also be seen in Fig. 19. Significantly higher TIs were observed for the specimens reinforced by the fibres with the highest aspect ratio, UHSPE-1000 fibres of 1.905 cm lengths, in comparison to all other fibre aspect ratios. Wang [18] reported increased abrasion with increased distance of slippage in fibre pull-out for specimens of nylon and polypropylene fibres within a concrete matrix. Increasing the amount of abrasion on the surface essentially increases the force needed for fibre slippage through the matrix. In an earlier paper [13] we reported that the analysis of the frictional forces in fibre pull-out could be performed by comparing the curve to the condition $d\tau_i/ds = 0$ (where τ_i = interfacial-shear strength, and s = slippage distance). In the examination of the fracture toughness curves obtained from the three-point bend loading test, it is apparent that for the specimens reinforced with the fibre aspect ratio of 776, $d\tau_i/ds > 0$ (Fig. 15c). Thus, the increase in frictional forces was not solely attributed to an increase in slippage distance for longer fibres. The shorter fibre lengths exhibited curves that were of the nature $d\tau_i/ds < 0$. It was not apparent from the SEM photomicrographs, whether or not the longer fibres had a larger density of plastic flow; but, it is safe to say that with the longer fibres there is a higher probability of plastic flow along the fibre length. Clearly, the longer fibres gave a significant improvement in the reinforcement properties of the cements in comparison to the shorter fibres.

In comparing the other three fibre aspect ratios, it was found that for the fibre aspect ratio of 244, UHSPE-1000 fibres (6.35 mm), had a significantly higher TI in comparison to those with a fibre aspect ratio of 188, UHSPE-900 fibres (6.35 mm). No other statistically significant differences were observed.

TABLE VIII Toughness index means as a function of fibre aspect ratio (values are combined for virgin and plasma-treated fibres and weight fractions)

Fibre aspect ratio	Toughness index	CV (%)
0	1.00[a]	–
188	2.40[b]	25.0
244	3.02[c]	34.7
372	2.81[b, c]	21.5
776	4.37[d]	16.0

[a–d] The different letters represent significantly different means at $\alpha = 0.05$.

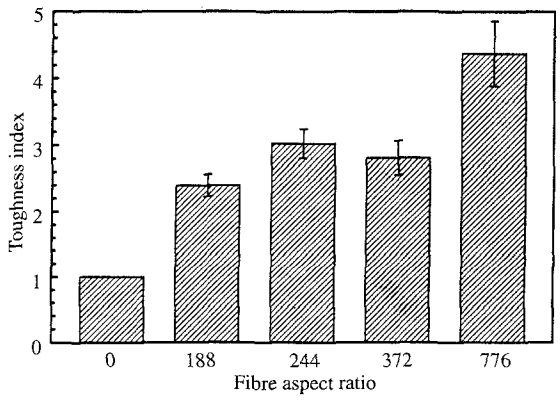

Figure 19 Toughness index (means ± one standard error) as a function of the fibre aspect ratio (values are combined for all virgin and plasma-treated fibres, and for all weight fractions).

Since the UHSPE-1000 fibres have a smaller cross-sectional area than the UHSPE-900 fibres, and the fibres were the same lengths and densities, there were a larger number of UHSPE-1000 fibres within the matrix in comparison to UHSPE-900 because the amount of fibres used in the matrix was based on the weight fraction of PMMA powder to fibre. It was reported above that the weight fraction was a significant factor in determining the TI of the reinforced cements, so it is possible that the larger number of UHSPE-1000 fibres caused a significant improvement in the TI of the bone cements. No statistically significant differences were observed between the fibre aspect ratios of 244 and 372, UHSPE-900 fibres (12.75 mm). The combination of longer UHSPE-900 fibres and the larger amount of fibres within the matrix of the shorter UHSPE-1000 fibres, may have balanced the frictional forces, so that no statistical differences were observed between these two fibre aspect ratios.

4.6. Toughness index as a function of the plasma gas by fibre-aspect-ratio interactions

A summary of TI as a function of the interaction between fibre aspect ratios and the plasma gases is given in Table IX. All pairwise comparisons are given in the table, but only a select few of these will be discussed. The means (± one standard error) can be found in Fig. 20.

As can be seen by the pairwise comparisons, the cements with the highest aspect ratio of control fibres had a significantly higher TI than the shorter-length control fibres. This was not surprising, as the longer fibres of UHSPE-1000 within the matrix have a higher probability of containing surface flaws. The flaws would cause the fibres to be more susceptible to the prevention of slippage through the matrix.

The bone cements containing carbon dioxide treated fibres at the highest fibre aspect ratio had significantly higher toughness indices than all other specimens, except when compared to the cements reinforced with nitrogen treated fibres of the highest aspect ratio. This was not surprising, as the oxygen-rich

TABLE IX Toughness index means as a function of the interaction of fibre aspect ratios with the gas (values are combined for virgin and plasma-treated fibres)

Gas	Fibre aspect ratio l/d	Toughness index	CV (%)
No fibre	0	1.00[a]	–
Control	188	2.11[b]	20.3
	244	2.16[b, c]	22.0
	372	2.28[b]	25.3
	776	3.17[d, e, f]	27.5
Argon	188	2.57[b, c, d, e]	26.9
	244	3.42[f, g]	31.1
	372	3.04[c, d, e, f]	28.0
	776	4.10[g, h]	5.41
Carbon dioxide	188	2.36[b, c, d]	24.7
	244	3.01[c, d, e, f]	27.2
	372	3.19[e, f]	29.0
	776	5.43[h, i]	44.3
Nitrogen	188	2.55[b, c, d, e]	42.4
	244	2.55[b, c, d, e]	20.0
	372	3.59[f, g]	16.9
	776	4.82[i]	30.9

[a–i]The different letters represent significantly different means at $\alpha = 0.05$.

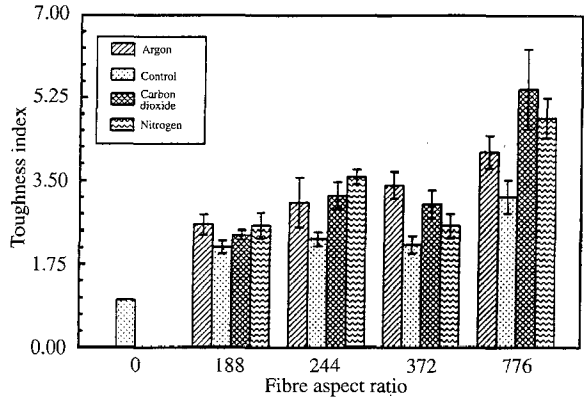

Figure 20 Toughness index (means ± one standard error) as a function of fibre aspect ratio and the plasma gas (values are combined for the two weight fractions).

environment is known to be a harsher treatment than other gases [11, 25, 26]. It is postulated that with the more rigorous treatment of carbon dioxide gases the fibres were probably more susceptible to plastic flow during slippage, causing the additional force needed for fibre pull-out.

4.7. Gas by fibre aspect ratio by weight fraction interactions

From the three-way analysis of variance of TI data, the three-way interaction of gas/fibre aspect ratio/weight fractions were found to have a probability level equal to 0.069, which was slightly above the set level of significance ($\alpha = 0.05$). However, there was reason to believe from the load–elongation curves that two of the treatments – specimens reinforced with carbon dioxide treated UHSPE-1000 fibres of 19.05 mm length at 1% weight fraction and nitrogen treated UHSPE-1000 fibres of 19.05 mm length at 1% weight fraction – were significantly higher than all other combinations. Thus, it was decided to perform a Student's *t*-test for all pairwise comparisons between these two combinations and all other combinations. Both the carbon dioxide and nitrogen-reinforced specimens of this combination were far superior to the other combinations in the measured toughness indices of these data.

Carbon dioxide and nitrogen are both reactive gases compared to argon, which is inert. The argon-plasma treatment of polyethylene films requires a much longer exposure time to obtain the same degree of wettability that is obtained in a few seconds with carbon dioxide or nitrogen gases [14]. It is probable that this same phenomena occurs in the fibres, although in our previous work we did not see these differences in fibre wettability among the three gases [14].

At least a sixfold improvement in the TI was seen in the cements reinforced with carbon dioxide treated UHSPE-1000 fibres of 19.05 mm lengths at 1 wt % compared to unreinforced cements. It is clear from these data that a significant improvement in the mechanical properties of the cements can be realized by reinforcing cements with carbon dioxide or nitrogen plasma-treated specimens with the longest fibres at the higher weight percentages of the treatments examined in this experiment.

5. Conclusions

We have conducted a study in the use of plasma-treated UHSPE fibres as a reinforcing phase in acrylic bone cements. The variables examined were weight fractions (0, 0.5 and 1%), fibre aspect ratios (l/d) (0, 188, 244, 372 and 776), and plasma gases (controls, argon, carbon dioxide and nitrogen). The following conclusions can be drawn from the data.

1. No significant improvement in flexural strength and only modest improvements in flexural modulus and the stress intensity factor were obtained by reinforcing the cements with surface-modified and virgin UHSPE fibres.
2. Significant improvements in the toughness index of fibre-reinforced cements were obtained by a *crack bridging* effect that occurs during the fibre pull-out process.
3. Significantly higher toughness indices were obtained in the cements reinforced with plasma-treated fibres than in the cements reinforced with virgin fibres. This is probably due to an increased susceptibility to plastic flow of the plasma-treated fibres during the fibre pull-out process. All specimens showed signs of plastic flow, as seen by SEM.
4. Significantly higher toughness indices were obtained in the cements reinforced with 1% weight fraction of fibres in comparison to those with 0.5%.
5. Significantly higher toughness indices were obtained in the cements reinforced with fibres of fibre aspect ratio 776.
6. At least a sixfold improvement in the toughness index (fracture energy) was observed by reinforcing the cements with carbon dioxide treated fibres with a fibre index (l/d) of 776 at 1% weight fraction.

Based on these data it appears that the plasma treatment altered the fibre surface sufficiently to cause significant differences in the susceptibility to plastic flow during the fibre pull-out process. The carbon dioxide treatment, noted as a more aggressive gas in the plasma chamber due to the high oxygen content, may have caused the fibres subjected to this treatment to be more susceptible to plastic flow than the other fibres during fibre pull-out. The fibres with a fibre aspect ratio of 776 had the longest fibres, 19.05 mm. The longer fibres had a higher probability of forming plastic flow along the fibre length, which coupled with the higher weight fraction could account for the higher energies observed in these particular specimens. All of the fibres added reinforcement by a *crack bridging* effect that significantly improved the toughness index compared to the non-reinforced cements.

Acknowledgements

This work was funded in part by a grant from Small Grants Committee, College of Human Ecology Cornell University Agricultural Experiment Station Grant No. 329424. The fibres were provided by Allied-Signal. The acrylic bone cement was provided by the Zimmer Corporation. Annie Cheng, an undergraduate student, was responsible for some of the sample preparation and testing.

References

1. J. CHARNELY, *J. Bone Jt. Surg.* **42B** (1960) 28.
2. *Idem., ibid.*, **46B** (1964) 518.
3. T. A. GRUIN, G. M. McNEICE and H. C. AMSTUTZ, *Clin. Orthop. Relat. Res.* **141** (1979) 17.
4. "Orthopædic knowledge update I", *Amer. Acad. of Orthop. Surg.*, Chicago, IL, (1984).
5. B. H. POURDEYHIMI and H. D. WAGNER, *J. Biomed. Mater. Res.* **23** (1989) 63.
6. R. A. LATOUR and J. BLACK, *J. Mater. Sci.* **24** (1989) 3616.
7. O. S. KOLLURI, S. L. KAPLAN and P. W. ROSE, *Soc. Plast. Eng./Adv. Polym. Compos. '88* **1–8** (1988).
8. S. HOLMES and P. SCHWARTZ, *Compos. Sci. Technol.* **38** (1990) 1.
9. S. KAPLAN and P. ROSE, *ANTEC '88* (1988) 1542–5.
10. S. L. KAPLAN, P. W. ROSE, H. X. NGUYEN and H. W. CHANG, *33rd Int. SAMPE Sympos.* (1988) 551–9.
11. O. S. KOLLURI, S. L. KAPLAN and P. W. ROSE, *Soc. Plast. Eng./Adv. Polym. Compos. '88* **1–8** (1988).
12. Z. F. LI and A. N. NETRAVALI, *J. Appl. Polym. Sci.* **44** (1992) 333.
13. D. N. HILD and P. SCHWARTZ, *J. Adhes. Sci. Technol.* **6**(8), (1992) 879.
14. *Idem., ibid.*, **6**(8) (1992) 897.
15. S. TIMOSHENKO and J. N. GOODIER, "Theory of elasticity", (McGraw-Hill, New York, 1951).
16. R. W. HERTZBERG, "Deformation and fracture mechanics of engineering materials", (Wiley, New York, 1976).
17. H. D. WAGNER and D. COHN, *Biomaterials* **10** (1989) 139.
18. Y. WANG, "Mechanics of fiber reinforced cementitious composites", Unpublished doctoral thesis, Massachussetts Institute of Technology (1989).
19. M. R. PIGGOTT, *Polym. Compos.* **3**(4) (1982) 179.
20. J. SMOOK, W. HAMERSMA, and A. J. PENNINGS, *J. Mater. Sci.* **19** (1984) 1359.
21. P. SCHWARTZ, A. NETRAVALI and S. SEMBACH, *Tex. Res. J.* **56**(8) (1986) 502.
22. K. W. M. DAVY, S. PARKER, M. BRADEN, I. M. WARD and H. LADIZESKY, *Biomaterials* **13** (1992) 17.
23. B. POURDEYHIMI, H. H. I. ROBINSON, P. SCHWARTZ and H. D. WAGNER, *Annals Biomed. Engin.* **14** (1986) 277.
24. B. POURDEYHIMI, H. D. WAGNER and P. SCHWARTZ, *J. Mater. Sci.* **21** (1986) 4468.
25. N. H. LADIZESKY and I. M. WARD, *ibid.*, **24** (1989) 3763.
26. S. WU, "Polymer interface and adhesion", (Marcel Dekker, New York, 1982).

Received 25 November 1991
and accepted 5 January 1993